Computing and Informatics, Vol. 33, 2014, 1237–1268

PARALLEL COMPUTER SIMULATION OF FIRE IN ROAD TUNNEL AND PEOPLE EVACUATION

Peter Weisenpacher, Ján Glasa, Ladislav Halada
Lukáš Valášek, Viera Šipková

Institute of Informatics
Slovak Academy of Sciences
Dúbravská cesta 9
845 07 Bratislava, Slovakia
e-mail: {Peter.Weisenpacher, Jan.Glasa, Ladislav.Halada,
Lukas.Valasek, Viera.Sipkova}@savba.sk

Abstract. Advances in CFD (Computational Fluid Dynamics) and significant increase of computational power of current computers have led to widespread use of CFD in aerodynamics, fluid dynamics, combustion engineering and other academic disciplines. One of such disciplines is computer modelling and simulation of fire in human structures. Fire is a very complicated and complex phenomenon. Fire research deals with such processes as combustion, radiation, heat transfer, turbulence, fluid dynamics, and other physical and chemical processes. Several advanced fire and smoke simulation systems have been developed to solve various aspects of fire safety in various conditions and environments. In this paper, the use of parallel version of the CFD simulator FDS (Fire Dynamics Simulator) for the simulation of fire spread and smoke development in a short road tunnel is described. In order to study the impact of the computational domain decomposition on the accuracy and reliability of simulation results, several simulations of a chosen fire scenario ran on the HP blade cluster utilizing different numbers of processors. The obtained parameters of fire and smoke were used to investigate the influence of the fire on people evacuation in the tunnel with active ventilation for a given traffic situation.

Keywords: Computer simulation, tunnel fire, people evacuation, FDS+Evac, CFD, agent system, parallel calculation, fire safety

1 INTRODUCTION

Tunnel is generally a very complex and robust structure which requires enormous investment costs. Therefore, a high degree of protection is required for each tunnel in operation. However, the growth of the number of cars on roads and also the number of tunnels cause the growth of car incidents. One of the most destructive events in tunnel is fire of a car or a group of cars. Therefore, the interest to investigate possible course of fire in each tunnel is increasing.

There are different possibilities how to study the course of fire and its consequences. An important form of fire study is to prepare a fire as a full-scale or small-scale experiment with various measuring instruments. Full-scale experiment is a copy of a fire in real or very similar geometric dimensions. Small-scale experiment is a copy of a fire in reduced geometric dimensions with some other input variables included. Consistent analysis of obtained experimental data often helps to formulate laws and description of combustion products, their range and other fire properties. However, fire experiment in a tunnel in operation is very expensive because it would cause material damage and even lead to the tunnel failure. Moreover, tunnels differ from each other by their shape, spatial dimensions, slope, ventilation, and so on. For this reason, the results of a full-scale fire experiment in one tunnel cannot be automatically applied to another tunnel. Another possibility is to use theoretical laws and the knowledge about physical modelling of fire which can be used as a test or demonstration of fire in given tunnel utilizing the main advantage of this approach, the flexible use of different distributions of flammable materials in the tunnel and different fire scenarios.

At present, several physical models which are used for such purposes are available. They are based on CFD (Computational Fluid Dynamics) and are known as field models unlike zone models which separate compartment into two zones (upper and lower layer) only. On the other hand, field models separate the whole space into thousands or more of small cuboids (cells) which are associated into computational meshes. In each cell, the basic conservation laws of mass, momentum and energy are applied with the aim to fulfill the fundamental conservation equations and relevant physical and chemical laws. They are widely used for fire modelling and evaluation of consequences of fire in buildings, tunnels and other structures.

There are many different field models. For instance, FDS, JASMINE, PHOENICS and some others are very popular. They are generally accepted to investigate and test the fire dynamics, smoke and temperature distribution and other parameters of fire and its behaviour. As a result, a lot of articles have been published regarding the methodology, validation, verification and testing the reliability of computer fire models. Moreover, the organizations that develop computer fire models make a continual upgrade of program versions of their products. Computer fire simulation cannot completely replace well-prepared real fire experiments; however, it is still a unique, sophisticated, low-cost and feasible instrument for studying the fire course in different environments with excellent ability to define different input

conditions and fire parameters. Therefore, during the last decades the interest in computer fire simulation has significantly increased.

There are many papers which deal with different aspects of fire in tunnels. For example, important studies on fire in a full-scale as well as in a reduced-scale tunnel have been published [24, 21, 22]. In [46, 2, 45, 19], validation of computer simulation procedures for a full-scale fire test related to the Memorial Tunnel Fire Ventilation Test Program was analyzed. Very important issues are also the optimization of ventilation system and investigation of the effect of jet fans distribution and their position on fire in given tunnel [1, 44, 47]. A good overview of the state of the art of the tunnel fire research can be found e.g. in [3, 20]. In this paper, we use the actual parallel version of FDS (Fire Dynamics Simulator) for the simulation of fire in a short road tunnel. In order to study the impact of the computational domain decomposition on the accuracy and reliability of simulation results, several simulations of a chosen fire scenario ran on the HP blade cluster utilizing different numbers of processors.

Modelling of evacuation in fire conditions is also a complex, challenging problem. Most existing evacuation models employ an agent-based approach to the pedestrian crowd dynamics. Pedestrian crowds, like many self-organizing systems consisting of individual entities, show complex emergent modes of behaviour based on simple deterministic and non-deterministic principles followed by the individuals making up the population. The agent-based models give more realistic representation of pedestrian movement and allow to better elucidate subtle but important details of pedestrian behaviour. Several evacuation simulators have been developed utilizing cellular automata or social force model, for instance CAFE, FDS+Evac, STEPS, building EXODUS, Simulex and Pathfinder. These models represent various approaches to reproducing the effect of fire (e.g. reduced visibility, smoke toxicity and irritation, increasing temperature) on the walking speed of evacuees and their behaviour. However, only few papers deal with the simulation of people evacuation in case of tunnel fire (see e.g. the papers [20, 42, 41, 43]). In this paper, we demonstrate the use of FDS+Evac which allows not only to study the fire and smoke dynamics but also to analyse people evacuation and the conditions under which people are evacuated and the effect of ventilation in tunnel. Verification and validation of combination of the FDS fire simulator and its evacuation module, Evac (or combination of FDS output data with other existing systems developed for crowd dynamics simulation) is an important issue for tunnel fire research. As the length of existing tunnels often reaches 1 km and more, it is necessary to calculate the FDS simulation in parallel. However, the current 5.5.3 version of FDS shows some inaccuracies related to dividing the computational space into sub-spaces (computational meshes) when compared to sequential calculation. These inaccuracies can have an influence on people evacuation strategies and thus on the whole evacuation. That is why the study of this issue is of great importance.

The paper is organized as follows. The next section briefly describes basic information about FDS+Evac. Section 3 describes a fire scenario in a road tunnel and its simulation using FDS, where the focus is on investigation of the impact of parallel

calculation of the simulation on the reliability and accuracy of simulation results. The use of FDS+Evac for the simulation of people evacuation in the tunnel under fire conditions is also illustrated. In Section 4, the main conclusions are summarized and some concluding remarks are added.

2 FDS

The main features of FDS are described in [35, 34, 14]. FDS solves a form of conservation equations for low speed, thermally driven flow. Although it is focused mainly on smoke and heat transfer from fires, it also includes modules for physical and chemical processes like thermal radiation, pyrolysis, combustion of the pyrolysis products, conductive heat transfer and fire suppression by sprinklers. The basic set of conservation equations for conservation of mass, species, momentum and energy are used [35]:

$$\frac{\partial \rho}{\partial t} + \nabla . \rho \, \mathbf{u} = \dot{m}_b''' \tag{1}$$

$$\frac{\partial}{\partial t}(\rho Y_\alpha) + \nabla . \rho Y_\alpha \, \mathbf{u} = \nabla . \rho D_\alpha \nabla Y_\alpha + \dot{m}_\alpha''' + \dot{m}_{b,\alpha}''' \tag{2}$$

$$\frac{\partial}{\partial t}(\rho \, \mathbf{u}) + \nabla . \rho \, \mathbf{u} \, \mathbf{u} + \nabla p = \rho \, \mathbf{g} + \mathbf{f}_b + \nabla . \tau_{ij} \tag{3}$$

$$\frac{\partial}{\partial t}(\rho \, \mathbf{h}_s) + \nabla . \rho h_s \, \mathbf{u} = \frac{Dp}{Dt} + \dot{q}''' - \dot{q}_b''' - \nabla . \dot{q}'' + \varepsilon, \tag{4}$$

where $\dot{m}_b''' = \sum_\alpha \dot{m}_{b,\alpha}'''$ is the production rate of species by evaporating droplets or particles; ρ is the density; $\mathbf{u} = (u, v, w)$ is the velocity vector; Y_α, D_α, and $\dot{m}_{b,\alpha}'''$ are the mass fraction, diffusion coefficient, and the mass production rate of α^{th} species per unit volume, respectively; p is the pressure; $\mathbf{f}_b$ is the external force vector; τ_{ij} is the viscous stress tensor; $\mathbf{h}_s$ is the sensible enthalpy; and $\mathbf{g}$ is the acceleration of gravity. The term $\dot{q}'''$ is the heat release rate per unit volume from a chemical reaction and $\dot{q}_b'''$ is the energy transferred to the evaporating droplets. The term $\dot{q}''$ represents the conductive and radiative heat fluxes. Note that $D()/Dt = \partial()/\partial t + \mathbf{u}.\nabla()$. To these four equations, the equation of state for a perfect gas

$$p = \frac{\rho R T}{\bar{W}}, \tag{5}$$

in which R is the universal gas constant, T is the temperature and $\bar{W}$ is the molecular weight of gas mixture, is added. The pressure equation is obtained by taking the divergence of the momentum equation,

$$\nabla^2 H = -\frac{\partial \nabla . \mathbf{u}}{\partial t} - \nabla . \mathbf{F}. \tag{6}$$

In this equation the value H represents the total pressure divided by the density and vector $\mathbf{F}$ represents the convective and diffusive term in the momentum equation.

Finally we obtain a system of equations for these unknowns: the density ρ, three components of the velocity $\mathbf{u} = (u_1, u_2, u_3)$, temperature T, pressure p and mass fractions Y_α; all functions of three spatial dimensions and time. These equations must be simplified, in order to filter out sound waves, which are much faster than typical flow speed in fire conditions. Final numerical scheme is an explicit predictor-corrector finite difference scheme, which is second order accurate in space and time. The variables are updated in time using an explicit second-order Runge-Kutta scheme. The Poisson equation (6) for modified pressure is solved in every time step by a direct FFT-based solver that is a part of the CRAYFISHPAK library. Boundary conditions are prescribed on the walls and vents.

All input data for a simulation are conveyed in the form of a text file in prescribed format, which describes the coordinate system, geometry of the domain and its location in the given coordinates, mesh resolution, obstructions and their material properties, vents, boundary conditions, and different simulation parameters, including desired output quantities. An important limitation of the program is that the domain must be rectilinear, conforming with the underlying grid. The domain is filled with rectangular obstructions representing real objects, which can burn, heat up, conduct heat, etc. Describing their burning parameters properly is probably the most challenging task for the user. Simulation output includes quantities for gas phase (temperature, velocity, smoke volume fractions, visibility, pressure, heat release rate per unit volume, etc.), for solid surfaces (temperature, heat flux, burning rate) as well as global quantities (total heat release rate, mass and energy fluxes through openings, etc.). During the simulation, these outputs are saved in prescribed format in the output files and some of them can be visualised by the Smokeview program [7].

The aim of FDS is to solve practical problems in fire protection engineering as well as to provide a tool to study basic processes in combustion and fire dynamics. It is well known that the accuracy of simulating fires highly depends on the grid resolution. Therefore, in many papers authors investigate effects of the grid resolution on the different fire parameters, such as the flame height, radiative heat fluxes, temperature distribution and so on. Another serious problem is computation of the total pressure value H which fulfills Equation (6). The numerical scheme solving this Poisson equation is based on a fast Fourier transform (FFT). The precision of this solution is very important and has a marked influence on simulation outputs. During the last years, a parallel version of FDS, which makes possible to use this simulation program also for simulation of fire in large areas such as buildings, garages, tunnels, and so on, has been available. It is not surprising that the decomposition of large computational domain on tens or much more sub-domains requiring mutual communications is also a problem which must be thoroughly analysed. Especially, the coupling of the pressure solver across the mesh boundaries in a multi-mesh simulation must be tested and verified. Our analysis presented in this paper confirms that the different scalability of computational domain has an influence on the computed value of temperature and consequently also on another output quantities.

A similar result has been published in other papers [33, 6]. It is very important to develop a new parallel concept for the pressure equation because in the actual parallel version FDS 5.5.3 it does not meet the basic requirement of the physical principle on which it is based on, that the pressure at every point of experimental space depends on the pressure in all other points of this space including the boundaries of the whole domain. This principle is not successfully applied in the current FDS version. Thus, the error of the pressure value has an influence on the precision of the temperature and other output quantities.

2.1 Realization of FDS Simulations

The FDS model has been developed to run on a variety of platforms, and operating systems MS Windows, Mac OS X, and Unix/Linux. To effectively exploit all available computing resources with the view of gaining the best performance, FDS supports the configuration of four programming models.

A *sequential model* is designed for running on a single CPU. A *parallel MPI model* is designed for running on distributed memory systems, e.g. a computer cluster. To execute FDS as a single parallel job on a distributed memory system, the MPI (Message-Passing Interface) [38] is applied. The main strategy consists in decomposition of the computational domain into multiple meshes and computation of the flow field in each mesh performed as an individual MPI process. MPI routines handle the transfer of information between these processes. Usually, each mesh is assigned to its own MPI process, but it is also possible to allocate multiple meshes to a single MPI process. In this way, large meshes can be computed on dedicated processors, while smaller meshes can be grouped together in one process running on a single processor. A *multi-threading OpenMP model* is designed for running on shared memory systems, e.g. a multi-core CPU. FDS multi-threading is implemented through the OpenMP library [37], which allows the concurrent execution of multiple threads within the context of a single process. It enables to employ all available processors or cores on a given machine. A *hybrid MPI & OpenMP model* is designed for running on distributed shared memory systems, e.g. an HPC multi-core cluster, which may include a shared memory between cores within a node, and a distributed memory between nodes. The combination of MPI and OpenMP approaches enables to apply a two-level parallelization: first the computational domain is decomposed into multiple meshes for distributed memory (MPI), and then within each mesh the multi-threading on some selected code regions is used for shared memory (OpenMP).

For simulations referred to in this paper, the FDS package version 5.5.3 was utilized. All programming models were compiled by means of GNU compilers version 4.4.6 (gcc, gfortran, OpenMP) and Open MPI version 1.4.

FDS simulations of real fire scenarios represent long-time, computationally intensive, and memory consuming jobs. Experiments were carried out on the local HPC cluster using the PBS (Portable Batch System) [39], and also on the grid infrastructure EGI (European Grid Infrastructure) [4] using the EMI 2 [5] grid middleware.

2.1.1 Running FDS on Local Cluster

The HP blade cluster employed is located at the Institute of Informatics, Slovak Academy of Sciences, Bratislava. It consists of 54 compute nodes, each comprising of two 6-core 2.4 GHz processor Intel Xeon X5645 and 48 GB of RAM. All nodes are connected by the Infiniband interconnection network with the bandwidth of 40 Gbit/s per link and direction.

To submit and start a batch job on a computer cluster the qsub command is used, to which a job submission script is passed as argument. Typically, the job submission script for the PBS server represents a Shell script including PBS commands. A number of options on qsub allow the specification of attributes which may affect the behavior of the job execution. The sequential model of FDS is executed on one processor-core. The OpenMP model of FDS is executed on one node, where the number of threads may range from two to the maximum number of cores per node. When running the MPI model of FDS, MPI processes are allocated by default applying the *slots-strategy*, where one MPI process is launched per processor core. It is also possible to launch MPI processes one per node (*nodes-strategy*), cycling by node in a round-robin fashion. When running the hybrid MPI & OpenMP model of FDS, MPI processes are launched using the *nodes-strategy*, where each node has a sufficient number of cores available (free cores are reserved to fork OpenMP threads).

2.1.2 Running FDS on Grid Infrastructure

All FDS models were ported into grid infrastructure EGI [4]. Jobs to be executed on the grid are described in the language JDL (Job Description Language) [23]. JDL represents a flexible, high-level language based on the Condor classified advertisement, which enables to describe jobs and aggregates of jobs with arbitrary dependency relations, and to express any requirements and constraints on the computing and storage resource.

EGI operates using the grid middleware EMI 2 (Matterhorn) [5]. For the submission of a job to EGI the client command glite-wms-job-submit is used, to which a job description in JDL is passed as input argument. Commands glite-wms-job-status and glite-wms-job-output are used for monitoring the status of submitted jobs and retrieving a possible output of finished jobs.

The invocation of the actual FDS executable is done within a wrapper script which also handles the post-processing of output data files. MPI and MPI & OpenMP models of FDS are initialized by means of the MPI-Start [36] representing an abstract software layer that offers a unique interface to the grid middleware to start MPI programs with various execution environments implementations. MPI-Start is a fixed part of the EMI 2 middleware.

2.1.3 FDS Running Support

In order to facilitate the process of simulation runs, for each FDS model we have developed a supporting tool – a pair of *fds-master* scripts written in Shell, which provide for the fully automatic submission of FDS jobs to the local cluster or to EGI. Each of the *fds-master* scripts accomplishes the following actions. It accepts and checks input arguments specifying the FDS input file, and required running configuration (the number of nodes, the number of cores, and eventually, the number of MPI processes and number of threads); arguments are passed to the subsequent operations. Based on given input arguments, it produces the corresponding *fds-submission* script which serves as the input to the qsub command in case of running FDS on the local cluster, or to the glite-wms-job-submit command in case of running FDS on EGI. Finally, it provides for the execution of the FDS simulation using the previously generated *fds-submission* script. From the user point of view the realization of the FDS simulation represents the call of the *fds-master* script with needed input parameters.

2.2 FDS+EVAC

FDS+Evac [25] is a combined agent-based egress calculation model and a CFD model of fire-driven fluid flow, where the fire and egress parts interact. The evacuation module of FDS was developed and is currently maintained by VTT Technical Research Centre of Finland. It is intended to the simulation of egress problem in fire conditions (fire evacuation), but can also be used just to simulate egress without any fire calculation (fire drill) [26, 28, 29, 30, 27].

FDS+Evac treats each evacuee as a separate entity (agent), which has its own personal properties and escape strategies. The basic algorithm for modelling the agents movement solves an equation of motion for each agent in a continuous 2D space and time, doing some kind of an artificial molecular dynamics for agents. The model behind the movement algorithm is the social force model [18, 16, 17, 50] taking into account motive and physical forces, such as for instance contact forces, and psychological forces exerted by the environment and other agents. The model was modified to better describe the shape of the human body [32, 28, 29, 30, 27]. The integration of the evacuation calculation into the fire calculation allows to use the quantities relevant to fire to model the behaviour of evacuating people and the impact of fire onto their behaviour. Gas phase concentrations of O_2, CO_2, and CO are used to calculate Purser's Fractional Effective Dose (FED) index [40] indicating the human incapacitation. Smoke density affects the walking speed and the exit selection algorithm of the agents and speed up the detection of the fire [8]. The evacuation part of FDS+Evac is stochastic, i.e., it uses random numbers to generate the initial position and properties of the agents and add a small random force on each agent's equation of motion. All input parameters required by the evacuation module of FDS to describe a particular scenario are conveyed via the input FDS file. A complete description of the input parameters can be found in [25].

FDS+Evac computes the position, velocity and toxic gases dose of each agent inside the computational domain at each discrete time step. The movement of agents and selected quantities related to evacuation can be visualised by Smokeview [7]. Some other detailed information which include e.g. the initial positions and properties of the agents can be found in the diagnostic FDS+Evac output text file.

The shape of the human body is approximated by a combination of three overlapping circles. Each agent follows its own equation of motion (boldface is used for vector quantities):

$$m_i \frac{\mathrm{d}^2 \boldsymbol{x}_i(t)}{\mathrm{d}t^2} = \boldsymbol{F}_i^m(t) + \boldsymbol{F}_i^a(t) + \boldsymbol{F}_i^w(t) + \boldsymbol{F}_i^e(t) + \boldsymbol{\xi}_i(t), \tag{7}$$

where $\boldsymbol{x}_i(t)$ is the position of agent i at time t; m_i is the mass of agent i; $\boldsymbol{F}_i^m(t)$ denotes the motive force at time t; $\boldsymbol{F}_i^a(t)$, $\boldsymbol{F}_i^w(t)$, and $\boldsymbol{F}_i^e(t)$ denotes the agent-agent, agent-wall, and agent-environment interaction at time t, respectively; $\boldsymbol{\xi}_i(t)$ is a small random fluctuation force;

$$\begin{aligned}
\boldsymbol{F}_i^m &= \frac{m_i}{\tau_i}(\boldsymbol{v}_i^0 - \boldsymbol{v}_i), \\
\boldsymbol{F}_i^a &= \sum_{i \neq j} (\boldsymbol{F}_{ij}^s + \boldsymbol{F}_{ij}^c + \boldsymbol{F}_{ij}^a), \\
\boldsymbol{F}_i^w &= \sum_{w} (\boldsymbol{F}_{iw}^s + \boldsymbol{F}_{iw}^c) \\
\boldsymbol{F}_i^e &= \sum_{k} \boldsymbol{F}_{ik}^a,
\end{aligned}$$

$\boldsymbol{v}_i(t) = d\,\boldsymbol{x}_i(t)/dt$ is the velocity of agent i at time t; $\boldsymbol{v}_i^0$ is the value of agent's own specific unimpeded walking speed; τ_i is the relaxation time parameter determining the strength of the motive force which makes an agent to accelerate (for more details about the form of the particular components of the social, contact and attraction/repulsion agent-agent and agent-wall forces, see [25]).

The rotational movement of the agent i is described similarly by the rotational equation of motion

$$I_i^z \frac{\mathrm{d}^2 \varphi_i(t)}{\mathrm{d}t^2} = M_i^c(t) + M_i^s(t) + M_i^T(t) + \eta_i^z(t), \tag{8}$$

where $\varphi_i(t)$ is the angle of agent i at time t; the tensor I_i^z is the moment of inertia; $\eta_i^z(t)$ is a small random fluctuation torque; M_i^c, M_i^s and M_i^T are the torques of the contact, social and motive forces, respectively;

$$\begin{aligned}
\boldsymbol{M}_i^c &= \sum_{i \neq j} (\boldsymbol{R}_i^c \times \boldsymbol{F}_{ij}^c), \\
\boldsymbol{M}_i^s &= \sum_{i \neq j} (\boldsymbol{R}_i^s \times \boldsymbol{F}_{ij}^s);
\end{aligned}$$

and the motive torque is determined analogously as the motive force (for more details see [25]).

In FDS+Evac, agents are guided to exit doors using a preferred walking direction vector field calculated by the flow solver of FDS as an approximation to potential flow problem of 2D incompressible fluid in given boundary conditions, where walls and obstructions are inert and exit doors act as fans in FDS. A short range collision avoidance model is also included, where the area in front of the agent i is divided into three overlapping sectors. The algorithm selects the sector with the least counterflow; taking into account the agents' location and velocity. The exit selection is modelled as an optimization problem, where the exit that minimizes the evacuation time of the agent is selected taking into account the estimated walking time and estimated time of queueing. Other factors influencing the decision making process of the agent, such as the familiarity of the agent with an exit, the visibility of exits and the blocking effect of smoke and obstacles are also covered in FDS+Evac adding constraints to the evacuation time minimization problem.

The evacuation model briefly described above has been tested, validated and compared with various available egress models. The most significant benefit of using FDS as the platform of egress model is the direct and easy access to the fire related properties, such as gas temperatures, smoke and gas densities, and radiation levels at each point in the computational mesh. The FDS+Evac system is under intensive research and validation in order to increase the model accuracy and reliability and include new features and abilities of higher FDS versions.

Proper and easy modelling of phenomena related to the crowd dynamics, i.e., the behaviour of idividuals, crowds and groups of people in fire conditions is a complex, challenging problem in each evacuation simulator. In the following section, we show some simple examples of modelling of such behaviour for the case of fire evacuation in tunnel.

3 COMPUTER SIMULATION OF FIRE IN ROAD TUNNEL

In this section, we briefly describe a simple fire scenario in a full-scale model of a short, 2-lane road tunnel with two double jet fans. The fire which is to be modelled corresponds to a car fire with 10 MW total heat release rate.

The aim od this paper is not to optimize the tunnel ventilation system setting the critical velocity for the simulated fire scenario. We rather study the impact of parallelization of the calculation on the simulation accuracy and reliability. Therefore, we select a fire scenario which shows a more complex smoke behaviour in some parts of the tunnel. Some preliminary results of parallel simulation of tunnel fires summarized in this section have been published in [14, 48, 49].

3.1 Fire Scenario in Tunnel

Let us consider a 180 m long 2-lane road tunnel model with the dimensions of 10 m × 180 m × 7.2 m (see Figure 1). The tunnel ventilation system is longitudinal consisting

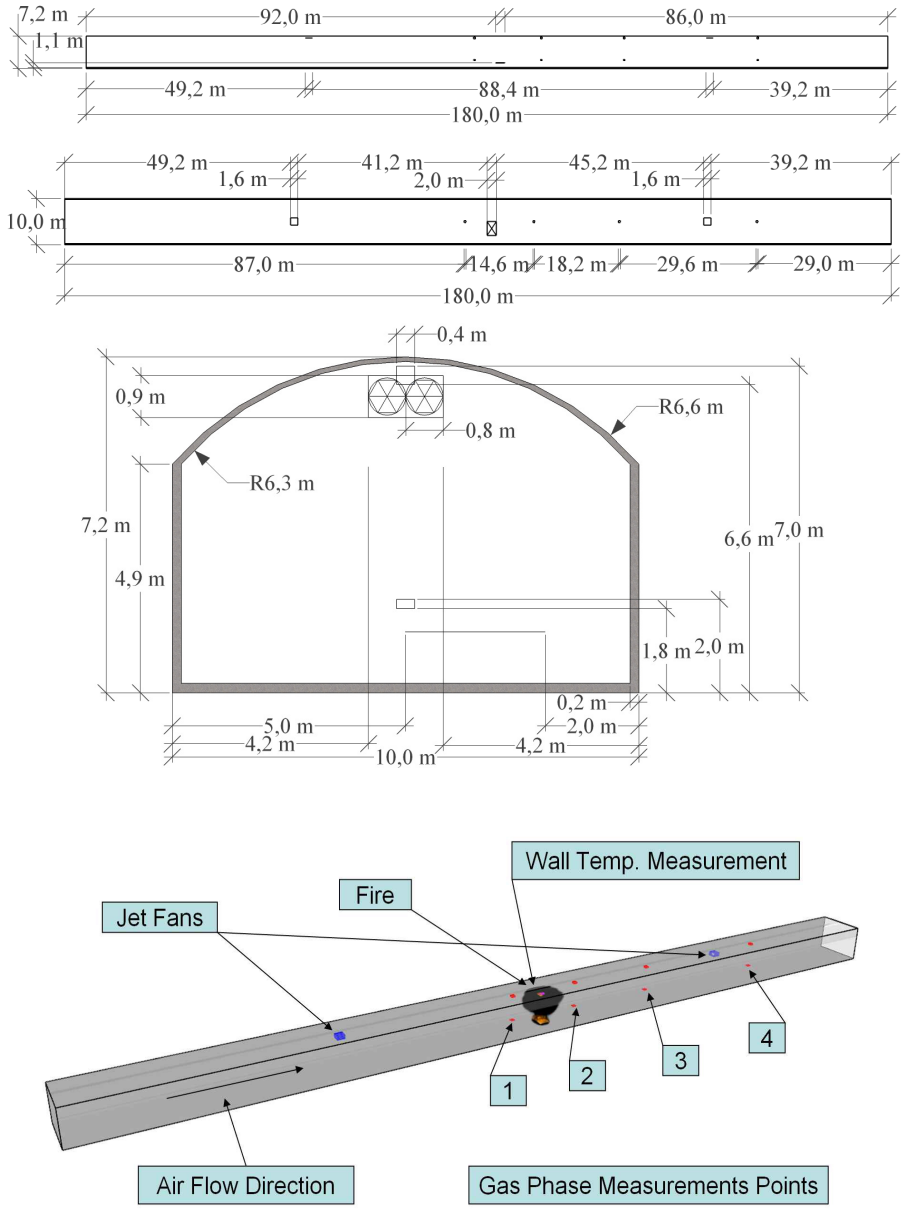

Figure 1. Tunel model and its FDS representation

of two double jet fans located under the ceiling at the distances of 49.2 m and 139.2 m from the left entrance of the tunnel, respectively.

We consider the initial fire source corresponding to an automobile fire. In simulation, it was represented by burning of a 2 m × 3 m plane placed 1.1 m above the floor at the 92 m distance from the left entrance of the tunnel (see Figure 1). The maximum heat release rate per unit area (HRRPUA) and the total heat release rate (HRR) of the fire was 1 666.67 kW/m^2 and 10 MW, respectively. The fire produced a large amount of smoke which was represented in simulation by setting up the soot yield parameter of the fire to 0.2. We assume that during the simulation the fire did not spread along the tunnel. That is why other flammable materials were not placed at any other places in the tunnel. In this part dealing with the parallelization investigation, no vehicles influencing the air flow in the tunnel were included. The ambient tunnel air temperature was set to 20°C. Total duration of simulation was 150 s.

We assume the following fire dynamics and jet fans operation. At time $t = 0$ s, both fans started to blow with the velocity of 5 m/s in the y direction. They worked for 50 s in order to ensure a steady air circulation in the whole tunnel. At time $t = 40$ s, the fire source was initiated with linearly increasing intensity till it achieved the 10 MW maximal HRR at time $t = 45$ s. Since that time, the fire intensity remained constant until the end of the simulation. At time $t = 50$ s (i.e., 10 s after the fire start), both fans started to increase their power linearly achieving 20 m/s (the maximal value of their velocity) at time $t = 55$ s. Since that time their velocity was not changed until the end of the simulation.

In order to record some selected quantities that were significant to further simulation results investigation, several control devices were placed in the simulation. Mean values of selected gas phase quantities (soot volume fraction, visibility, temperature and carbon monoxide mass fraction) were measured inside small testing volumes placed under the ceiling and at human head level (see Figure 1). Slices of the gas temperature, and oxygen and carbon monoxide mass fractions were recorded for several planes. The wall temperature of the tunnel ceiling was also determined at the place above the fire.

3.2 Paralellization of the Calculation and Simulation Results Analysis

We performed eleven variants of the simulation which differ from each other in the way how the computational domain was divided into particular computational meshes and in the number and size of cells used for calculation (see Table 1). Each computational mesh was assigned to one CPU core or thread.

The simulation 1 M, in which the computational mesh with the 10 cm resolution was used, is sequential. We use this simulation as a reference calculation and compare it with the parallel variants of the simulation performed. In the simulations 3 M, 4 M, 8 M and 24 M, the computational domain is divided regularly into 3, 4, 8 and 24 meshes in y direction, respectively, which have 10 cm resolution. In order to test the case in which the distance between the fire and the nearest mesh bound-

Simulation	Number of meshes: length in y direction (mesh resolution)
1 M	1 mesh: 180 m (10 cm × 10 cm × 10 cm)
3 M	3 meshes: 60 m (10 cm × 10 cm × 10 cm)
4 M	4 meshes: 45 m (10 cm × 10 cm × 10 cm)
8 M	8 meshes: 22.5 m (10 cm × 10 cm × 10 cm)
9 M	1 mesh: 7.5 m (10 cm × 10 cm × 10 cm) 7 meshes: 22.5 m (10 cm × 10 cm × 10 cm) 1 mesh: 15 m (10 cm × 10 cm × 10 cm)
10 M	1 mesh: 60 m (10 cm × 10 cm × 10 cm) 8 meshes: 7.5 m (5 cm × 5 cm × 5 cm) 1 mesh: 60 m (10 cm × 10 cm × 10 cm)
24 M	24 meshes: 7.5 m (10 cm × 10 cm × 10 cm)
48 M	48 meshes: 3.75 m (10 cm × 5 cm × 10 cm)
1 M*	1 mesh: 180 m (10 cm × 10 cm × 10 cm)
8 M*	1 mesh: 64 m (10 cm × 10 cm × 10 cm) 2 meshes: 8 m (5 cm × 5 cm × 5 cm) 4 meshes: 9 m (5 cm × 5 cm × 5 cm) 1 mesh: 64 m (10 cm × 10 cm × 10 cm)
3 M_L	1 mesh: 48 m (10 cm × 10 cm × 10 cm) 1 mesh: 60 m (10 cm × 10 cm × 10 cm) 1 mesh: 60 m (10 cm × 10 cm × 10 cm) → (10 cm × 14 cm × 10 cm)

Table 1. Computational domain partition: computational meshes description

ary is greater than in the other simulations, we consider the simulation 9 M, where the domain division is not regular. The meshes have the same 10 cm resolution. However, the meshes do not have the same number of cells (see Tables 1 and 2). The simulation 10 M includes two meshes (60 m long in y direction with 10 cm resolution) assigned to both side parts of the tunnel and 8 meshes (7.5 m long with

Simulation	MPI proc	OpenMP threads	CPU cores	Cells [mil]	Cells per mesh (max) [mil]
1 M	–	–	1	12.96	12.96
3 M	3	–	3	12.96	4.32
4 M	4	–	4	12.96	3.24
8 M	8	–	8	12.96	1.62
9 M	8	–	8	12.96	1.62
10 M	10	–	10	43.20	4.32
24 M	24	–	24	12.96	0.54
48 M	48	–	48	25.92	0.54
1 M*	–	8	8	12.96	12.96
8 M*	8	4	32	39.17	5.18
3 M_L	3	–	3	12.96	4.32

Table 2. Tunnel fire simulations characteristics

5 cm resolution) assigned to the 60 m central part of the tunnel. In the simulation 48 M, the domain is divided regularly in y direction into 48 meshes with resolution of 10 cm × 5 cm × 10 cm.

The simulations 1 M* and 8 M* are designed to study the performance and precision of the Open MP version of FDS. The 1-mesh and 8-mesh calculation is assigned to 8 and 32 Open MP threads (4 Open MP threads per one MPI process), respectively (see Tables 1 and 2). We tested also the performance of the linearly decreasing mesh resolution in the simulation $3M_L$ (see Tables 1 and 2).

In the sequel, we briefly summarize the obtained results for the described calculation parallelizations. For all cases, we calculate the measure D^*/δ, where D^* is the characteristic diameter of fire and δ is the grid size, which describes how well the flow field is resolved [35]. As $D^* = 2.4$ m, both the 10 cm and 5 cm mesh resolutions used in simulations could be considered as fine ($D^*/\delta > 10$).

The way of the computational domain division has a direct impact on the computational load and performance. The main computational characteristics of the simulation variants described above are summarized in Tables 2, 3 and 4.

In Table 2, the number of MPI processes, OpenMP threads per MPI process and CPU cores used in the particular simulation are specified. The information about the total number of cells and maximal number of cells per single mesh is also included.

Simulation	Time steps	Wall time [hrs]	Max CPU time per mesh [hrs]	Min CPU time per mesh [hrs]
1 M	33 041	377.2	375.8	375.8
3 M	31 905	172.4	169.5	165.6
4 M	32 839	130.9	128.6	125.5
8 M	31 277	68.2	67.2	63.2
9 M	30 947	69.8	68.9	–
10 M	60 727	313.6	309.6	289.4
24 M	31 206	32.6	32.0	26.9
48 M	68 759	63.2	61.5	53.8
1 M*	32 881	247.1	247.0	247.0
8 M*	60 054	203.8	199.2	194.1
3 M_L	31 358	150.9	149.8	145.5

Table 3. Tunnel fire simulations characteristics

Simulation	1 M	3 M	4 M	8 M	9 M	10 M	24 M	48 M	1 M*	8 M*	3 M_L
Speedup	1.00	2.19	2.88	5.53	5.40	1.20	11.57	5.97	1.53	1.85	2.50
c_{1M}/c	1.00	0.73	0.72	0.69	0.68	0.80	0.48	0.50	1.53	1.48	0.83

Table 4. Parallelization efficiency characterization

In Table 3, the number of time steps needed for the whole 150 s simulation calculation is shown. All processors operate in fully synchronized manner. This means that the simulation time step used for the integration of the system of partial differential equations that are to be solved is variable during the calculation; however, at given time it is the same for each particular computational mesh. The simulation time steps directly correspond to the mesh resolution. Therefore, the time steps in the simulations 10 M, 48 M and 8 M* (with 5 cm minimal resolution) are approximately one half of the values used for the rest of the simulations (see Table 3), whose resolution is 10 cm in all directions. That is why the number of parallel steps of the simulations with the 5 cm resolution is approximately two times larger than in the rest of the simulations. Consequently, the total execution time (see the values for the wall time and the CPU times per mesh in Table 3) is proportionally larger, while the number of cells also increases with finer resolution (compare with Table 2).

Taking into account these considerations and denoting the maximal cells number per mesh by N_{max} and the minimal mesh resolution by δ_{min}, we can assume that the overall simulation time depends on N_{max} and δ_{min} as follows [48]

$$t_{wall} = c.\frac{N_{max}}{\delta_{min}}, \tag{9}$$

where the parameter c involves all other influences such as e. g. a delay caused by communication between MPI processes. Comparing the value c obtained for all particular parallel simulations with the value c_{1M} for the sequential simulation, we can roughly characterize the efficiency of parallelization determining the ratio c_{1M}/c (see Table 4). The values of the speedup of all parallel simulations in comparison with the sequential calculation are also shown there.

The smoke development and the slices of the air flow velocity and temperature distribution in y direction at different time of the sequential simulation 1 M are shown in Figures 2, 3 and 4. The simulation illustrates the impact of ventilation on the course of fire. Smoke is slightly influenced by the steady air circulation in the first seconds after the fire start and then after the ventilation acceleration it is pushed away from the tunnel to the right part of the tunnel. Parallel simulations show qualitatively similar course of fire. They differ from the sequential simulation particularly in some quantities which capture local, highly variable characteristics of fire (such as the temperature, gas species volume fraction and others) at the places where intensive mixing of cold and hot gases appears. In the following, we focus on these differencies.

Figure 5 illustrates a comparison between the sequentional simulation 1 M and two parallel simulations which use 3 and 24 computational meshes. The gas temperature curves at the place at the right from the fire source (see Figure 1) show that the sequential simulation tends to reach larger values of temperature fluctuations in some phases of burning. However, the shape of the temperature curve corresponding to the sequential simulation seems to be smoother than the ones of

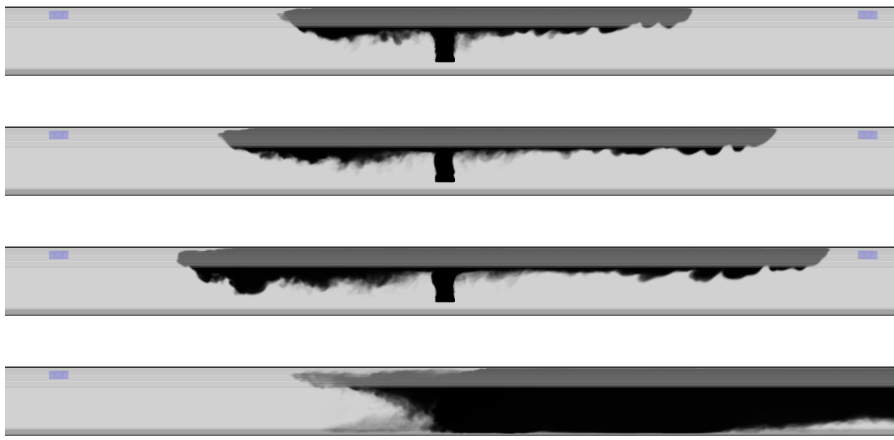

Figure 2. Smoke development in selected part of the tunnel at the 50^{th}, 53^{th}, 55^{th} and 137^{th} second of the simulation

parallel simulations (see Figure 5). It is probably due to the numerical approach used to resolve processes at boundaries of computational meshes. Nevertheless, the overall behaviour of all simulations is very similar (see the complete temperature curves in Figure 6).

Mesh boundaries have a similar effect on the simulation calculation as permeable barriers. They slightly slow down the heat transfer and smoke spread. In Figure 7, the temperature curves of the simulations 1 M, 3 M, 10 M, 24 M and 48 M related to the gas temperature at the farther place at the right from the fire source (see Figure 1) are shown. A noticeable delay of the temperature increase depending on the number of meshes in particular simulations can be observed (see Figure 7). The value of maximum delay is about 1 s (about 27 m far from the fire source). Although these delays affect the simulation accuracy, their effect is not critical. However, the impact of mesh boundaries on the computation precision is a nontrivial problem which requires further research [48].

The aim of the simulation 48 M analysis is to investigate the impact of deviation from cube meshes on the simulation results accuracy (see Figure 8). In 48 M, we used the 2 : 1 cells aspect ratio. It is not recommended to use too large values of the ratio because of the turbulence model implemented in FDS [35]. This is a probable cause of the physically not well-founded fluctuations which can be observed in the temperature curve just in the area, where a turbulent mixing of gases, which is caused by interaction of the ventilation and fire, occurs (see Figure 8).

The simulation 48 M has a substantially greater division of the computational domain compared with other simulations. However, the impact of this division on overall simulation results is not considerable (see the temperature curves of the simulations 1 M, 24 M and 48 M in Figure 9). This behaviour indicates that FDS can

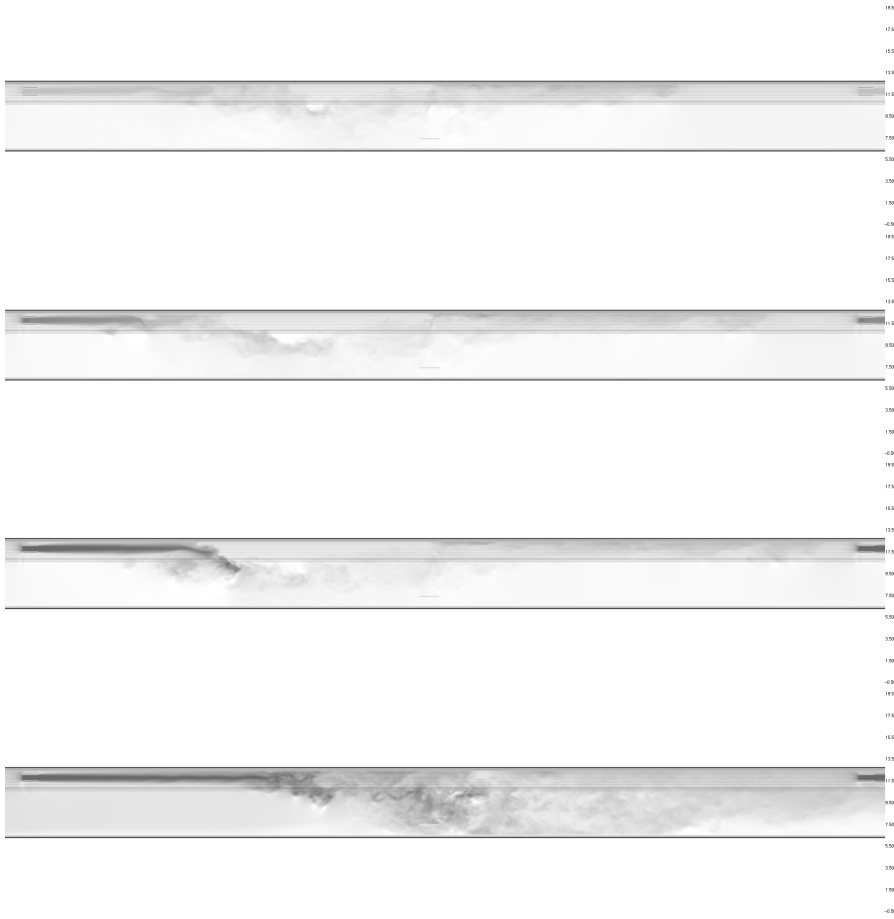

Figure 3. Slice of the air velocity in y direction in selected part of the tunnel at the 50^{th}, 53^{th}, 55^{th} and 137^{th} second of the simulation: the air velocity values represented by the grey level bar shown at the right vary from $-0.5\,\text{m/s}$ to $19.5\,\text{m/s}$

be used for long tunnel simulations with relatively high number of computational meshes to obtain reliable description of fire behaviour [48].

However, it is illustrated in Figures 10 and 11 that some quantities show a different behaviour for different parallel simulations. The problem is illustrated by the CO volume fraction (this problem requires further investigation) and wall temperature curves. A probable reason of the different behaviour of the wall temperature of the simulation 3 M in Figure 11 is the used finer mesh resolution (see also Tables 1 and 2). Nevertheless, the simulations provide reasonably rough estimates of these quantities [48].

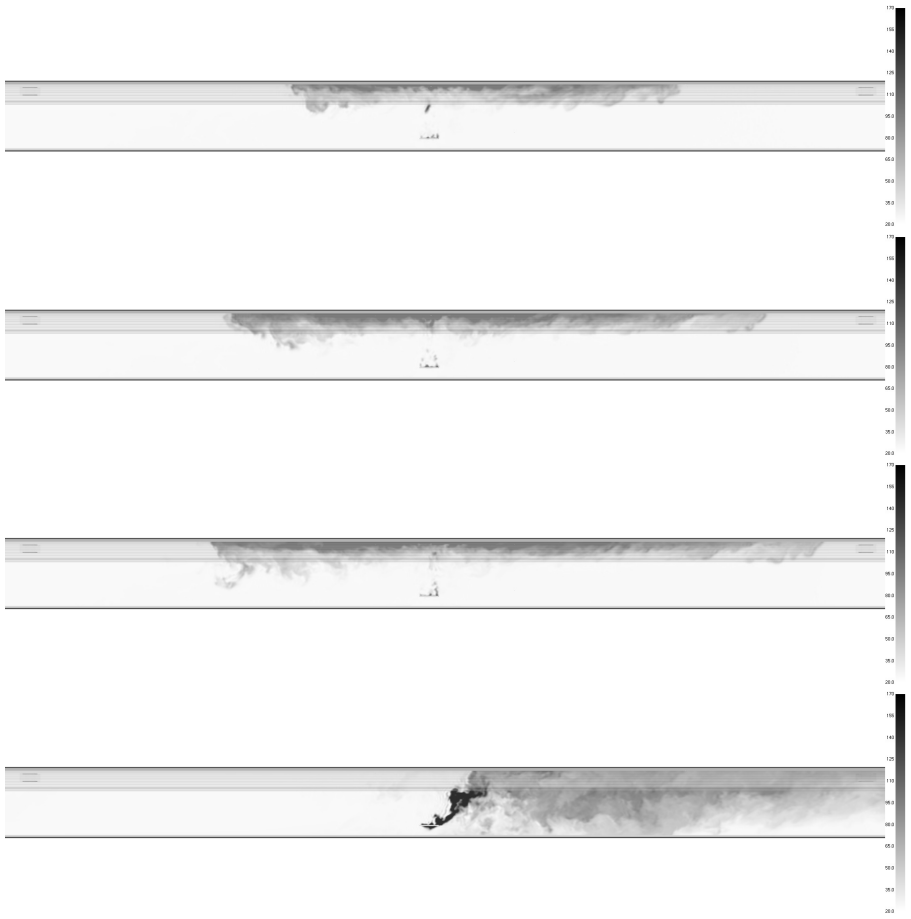

Figure 4. Temperature distribution in y direction in selected part of the tunnel at the 50^{th}, 53^{th}, 55^{th} and 137^{th} second of the simulation: the temperature values represented by the grey level bar shown at the right vary from 20^oC to 170^oC

3.3 People Evacuation in Tunnel

In this section, we use the tunnel fire described above to demonstrate the use of FDS+Evac for modelling a simple evacuation scenario. We insert traffic into the tunnel and consider the movement of people leaving vehicles in the tunnel as follows.

We follow the fire scenario described in the previous part (see Figure 2) considering steady air circulation in the whole tunnel by operating two double jet fans for the first 40 s. At time $t = 40$ s, the fire started achieving its total HRR at time $t = 45$ s as before. The fire ventilation operates since time $t = 50$ s as above. We consider 22 vehicles (two buses and 20 cars) and 116 persons in the scenario. Since

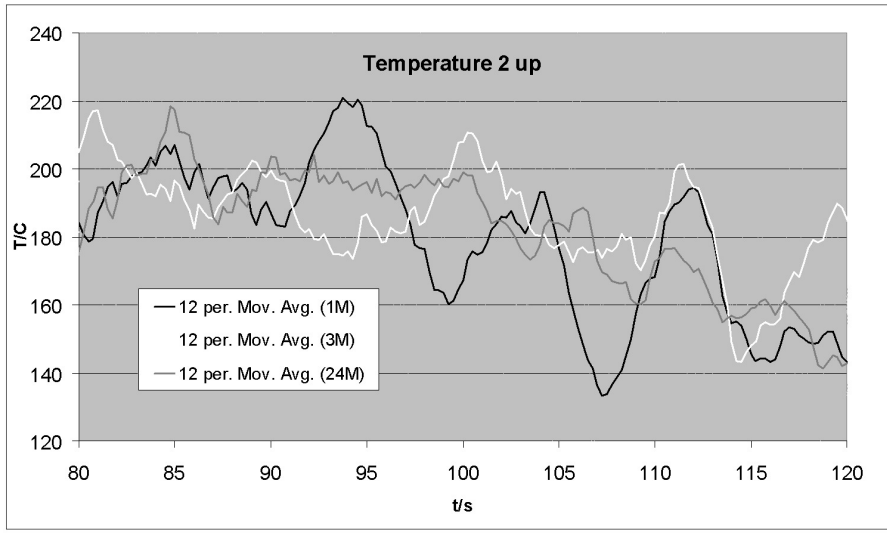

Figure 5. Comparison of temperature curves of the simulations 1 M, 3 M and 24 M: fragment of the curves

time $t = 43$ s, particular vehicles stop (are inserted into the simulation) at their positions according to Figure 12. Their arrival times are listed in Table 5. The time of the beginning of vehicles evacuation is set to 5 s after the vehicle stop. In Tables 6 and 7, the persons in particular vehicles and their evacuation time are specified, respectively.

Particular vehicle	B1	A1	A2	A3	B2	A4	A5	A6	...	A20
Arrival time [s]	43	44	45	46	47	48	49	50	...	64

Table 5. Arival time for particular vehicles in tunnel

We assume in the first evacuation scenario that passengers in all cars know (are familiar with) the tunnel portal through which they came into the tunnel (they saw the tunnel portal). At the right side of the tunnel at the distance of 73 m from the tunnel portal, there is a single 1.5 m wide exit door. We assume that it is visible from some of the first vehicles arrived. It is important to note here that we use the 2.3.1 version of FDS+Evac which still has its particularities that must be taken into account to set some parameters correctly. In this version, the same height (z-level) is assumed for the movement and for the visibility. At this level, the data affecting the agents behaviour (smoke and FED information) and the information about obstacles inhibiting agents from movement (walls, cars, buses) are collected. The points associated with exits (exit signs) used in the exit door selection algorithm (to decide if an exit is visible or not) are also considered as placed at that level. However, the current version of FDS+Evac does not distinguish between

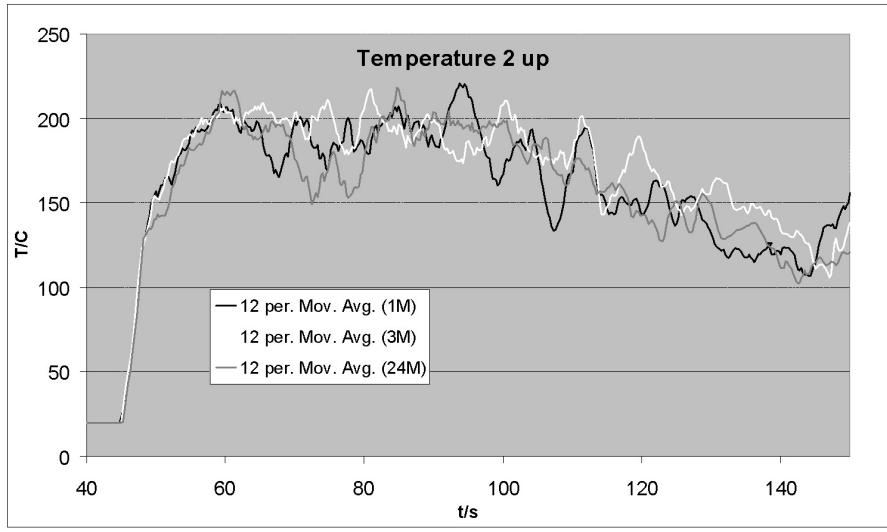

Figure 6. Comparison of temperature curves of the simulations 1 M, 3 M and 24 M

	B1	A1	A2	A3	B2	A4	A5	A6	A7	A8	A9
LFD	–	1 A	1 A	1 A	–	1 A	1 M	1 M	1 M	1 M	1 M
RFD	10 A	1 A	1 E	1 A	–	1 A	1 A	1 A	1 A	1 A	1 A
LBD	–	1 CH	–	1 CH	–	–	–	1 M	1 M	–	1 M
RBD	20 A	–	–	1 CH	25 A	–	–	1 A	1 A	2 CH	–
	A10	A11	A12	A13	A14	A15	A16	A17	A18	A19	A20
LFD	1 M	1 M	1 M	1 M	1 M	1 M	1 M	1 M	1 M	1 M	1 M
RFD	1 A	1 A	1 A	1 A	1 A	1 A	1 A	1 A	1 A	1 A	1 A
LBD	1 M	1 M	1 M	1 M	1 M	1 M	1 M	1 M	1 M	1 M	1 M
RBD	–	–	–	–	–	–	–	–	–	–	–

Table 6. Scheme of persons in particular vehicles, where LFD is the left front door, RFD is the right front door, LBD is the left back door, RBD is the right back door, and M, A, E and CH means the passenger group types Male, Adult, Elderly and Child from FDS+Evac, respectively

high obstacles (walls, buses) and lower obstacles (cars). Both types of obstacles are supposed to inhibit agents from seeing exit doors. Therefore, to ensure the portal visibility through cars we represent it by three individual 2 m wide exit doors. This representation provides that the evacuees escaping in three streams in the direction to the portal can see the portal. It is necessary to represent the exit width of the portal taking into account restrictions of pedestrian flow caused by standing vehicles in the tunnel to set correctly the FDS flow solver calculating the direction vector field. In the first evacuation scenario, we assume that the passengers in the vehicles $A1$, $A2$, $A3$, $B1$ and $B2$ also know the exit door (they can see it).

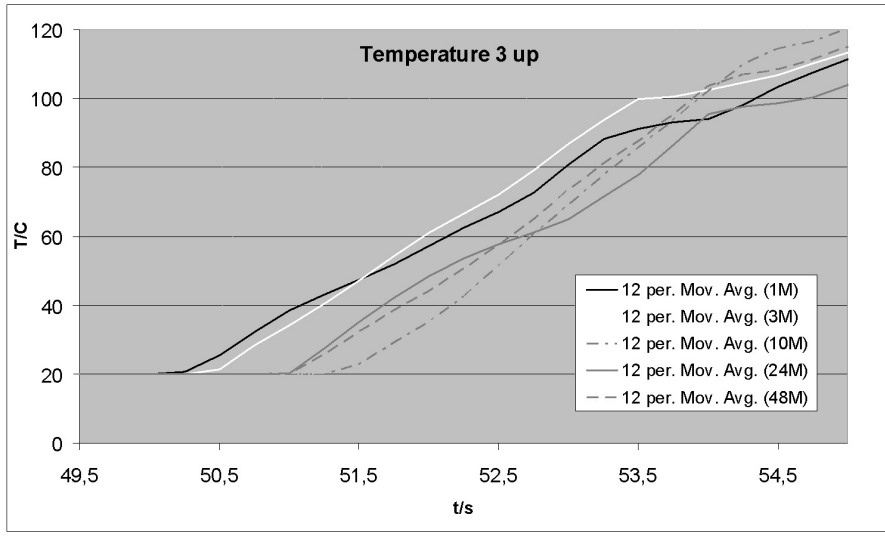

Figure 7. Impact of the domain division on the temperature time behaviour

	B1	A1	A2	A3	B2	A4	A5	A6	A7	A8	A9
LFD	–	49	50	51	–	53	54	55	56	57	58
RFD	48	49	51	51	–	53	54	55	56	57	58
LBD	–	49	–	51	–	–	–	55	56	–	58
RBD	48	–	–	51	52	–	–	55	56	57,58	–
	A10	A11	A12	A13	A14	A15	A16	A17	A18	A19	A20
LFD	59	60	61	62	63	64	65	66	67	68	69
RFD	59	60	61	62	63	64	65	66	67	68	69
LBD	59	60	61	62	63	64	65	66	67	68	69
RBD	–	–	–	–	–	–	–	–	–	–	–

Table 7. Scheme of the persons starting evacuation times (in seconds) in particular vehicles, where LFD is the left front door, RFD is the right front door, LBD is the left back door, RBD is the right back door

Figure 13 illustrates the course of evacuation at the 56^{th}, 66^{th}, 76^{th} and 86^{th} s of simulation. The evacuation started by the evacuation of the bus $B1$ at time $t = 48$ s. At the next seconds, the evacuation of other vehicles started (see Table 7). It follows from the analysis of this simulation that all passengers from the vehicles $B1$, $A1$, $A2$ and $B2$, as well as some of the passengers from the car $A3$ used the exit door placed at the right side of the tunnel. This exit door was the nearest available exit for escaping from the tunnel. The rest of passengers (two passengers from the car $A3$ and all passengers from the cars $A4$–$A20$) used the tunnel portal. The total evacuation time was 122.8 s.

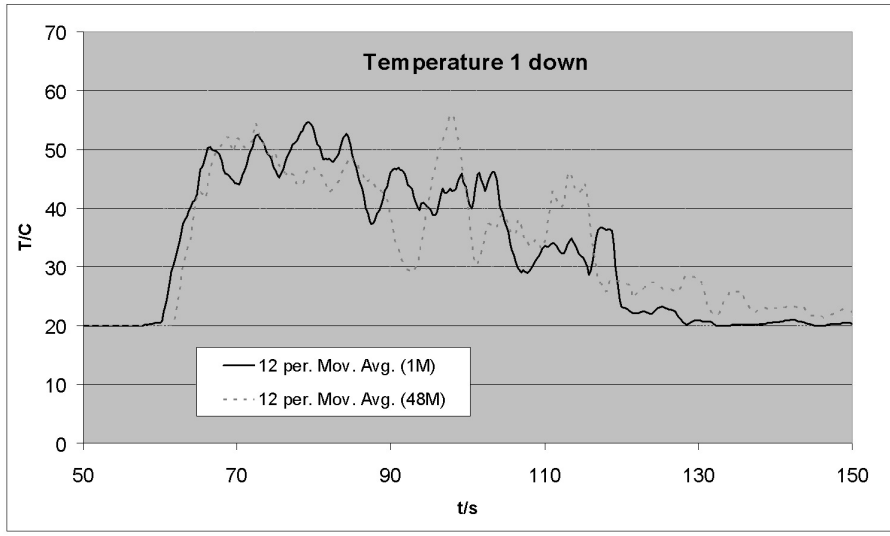

Figure 8. Comparison of the simulation 48 M with the sequential simulation

In Figure 14, the evacuation of four passengers from the car $A3$ is highlighted. They move in couples of the Adult-Child type. The picture shows the situation of the evacuation at the 51^{th}, 56^{th}, 59^{th} and 61^{th} s. One can easily see that the couple getting out from the left side door escaped using the tunnel portal while the couple from the right side door used the exit door for evacuation.

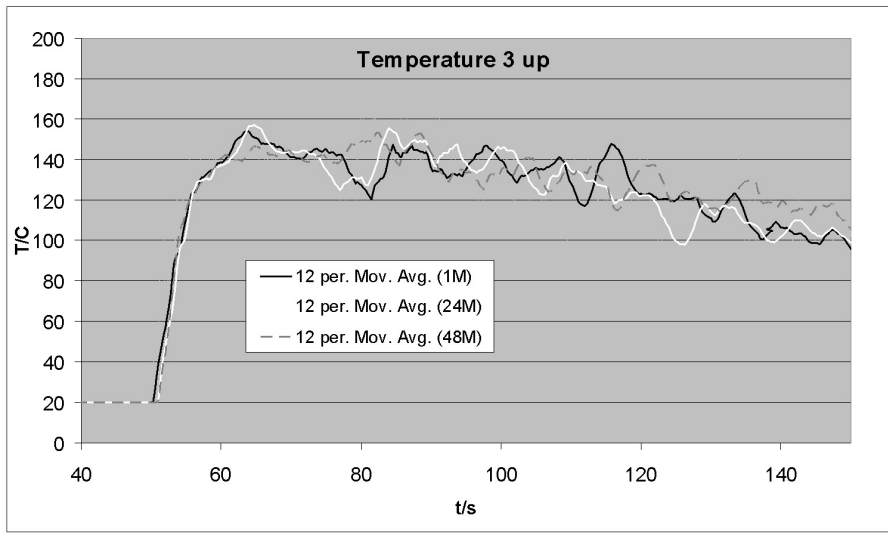

Figure 9. Temperature curves of the simulations 1 M, 24 M and 48 M

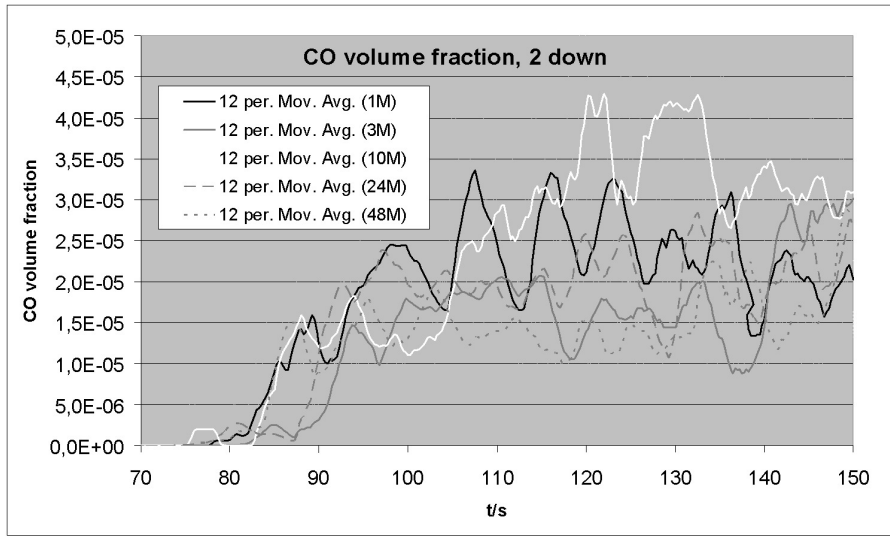

Figure 10. CO volume fraction above the fire source

However, there are situations in which the passengers from a given vehicle move and escape as a single group (for instance members of a family). FDS+Evac allows to set the agents inserted into evacuation to show such behaviour.

Figure 15 illustrates such evacuation scenario in which all passengers from the car *A*3 escaped through the exit door. Such behaviour was achieved by setting the

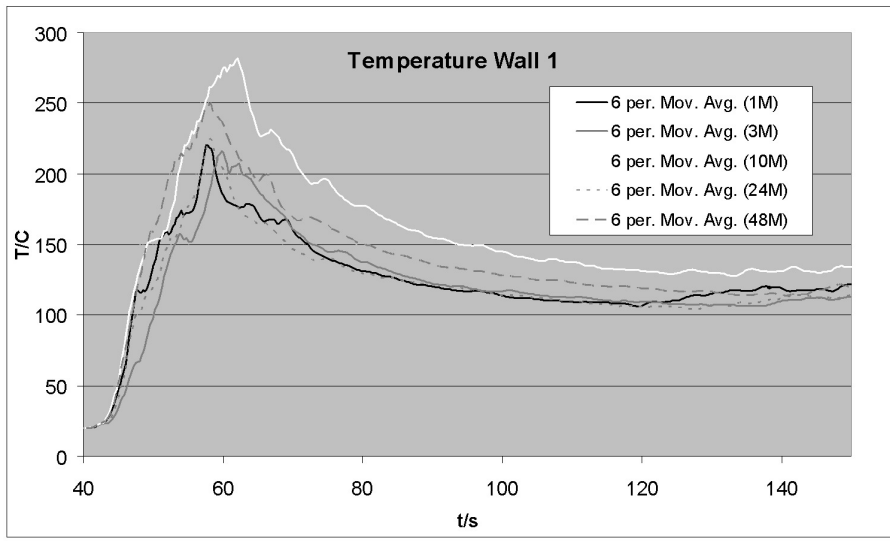

Figure 11. Wall temperature above the fire source

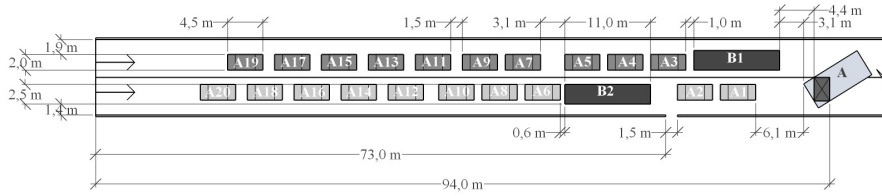

Figure 12. Scheme of traffic situation in tunnel: stopped vehicles positions

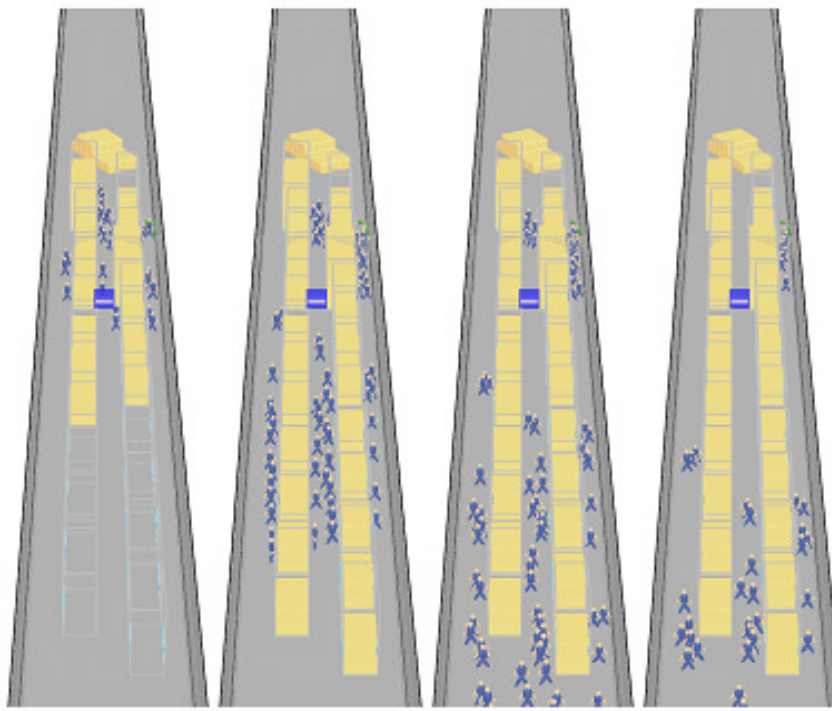

Figure 13. Course of evacuation at the 56^{th}, 66^{th}, 76^{th} and 86^{th} s

passengers from the car $A3$ to know (be familiar with) the exit and move according to the exit direction flow field. It can be observed in Figure 15 that both couples showed an autonomous movement to the exit. The total evacuation time was 126.6 s.

For more reliable movement of groups of evacuees, FDS+Evac is able to model the group behaviour involving group forces into the evacuation calculation. However, the existing model implemented in the current FDS+Evac version does not allow to insert members of a group into evacuation at different time and supposes that the whole group is inserted into the evacuation at the beginning of the calculation. Moreover, all members of a group must have the same personal properties. Note

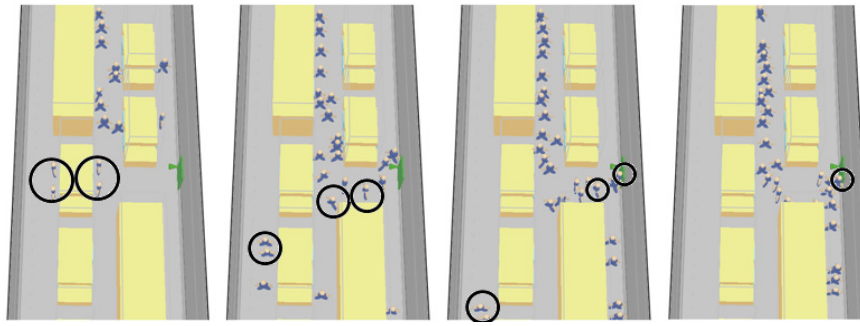

Figure 14. Course of evacuation of the passengers from the car $A3$ at the 51^{th}, 56^{th}, 59^{th} and 61^{th} s

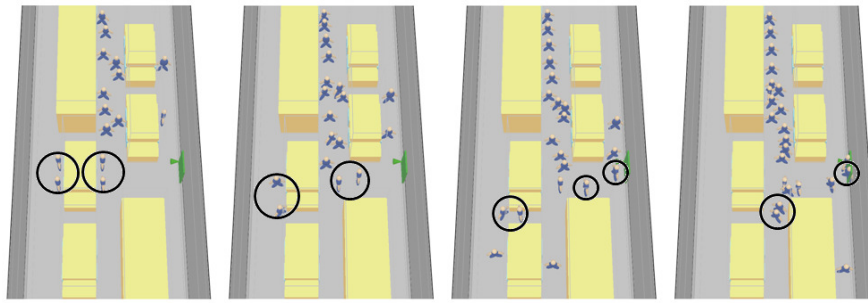

Figure 15. Course of evacuation of the passengers from the car $A3$ at the 51^{th}, 53^{th}, 54^{th} and 57^{th} s

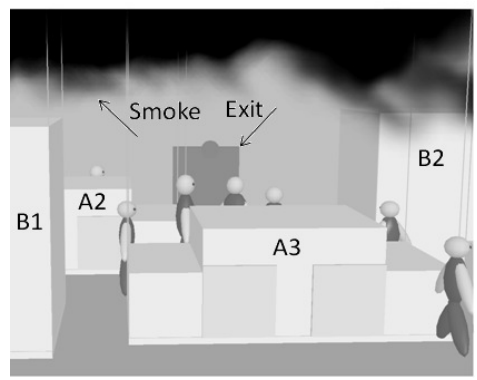

Figure 16. Fragment of evacuation at the 54^{th} s

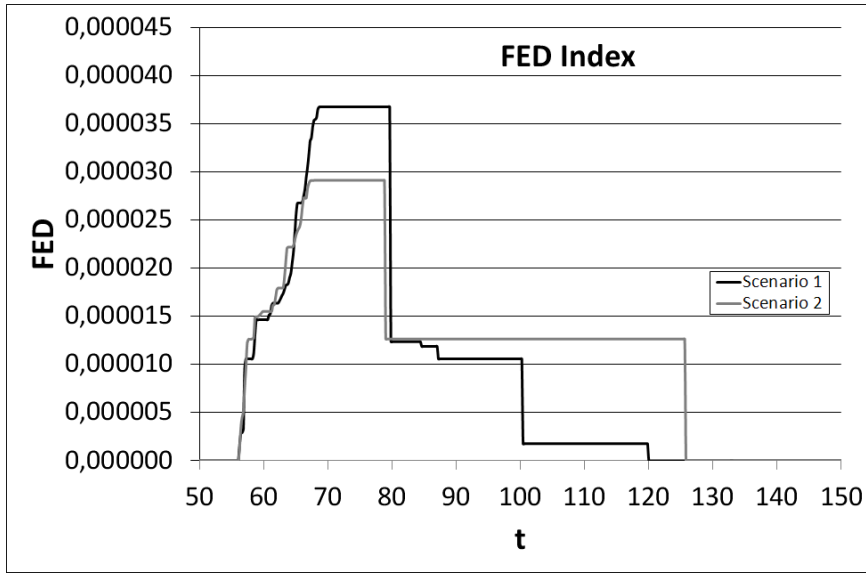

Figure 17. FED index curves for two evacuation scenarios

that a better treatment of the group force as well as the use of two z-levels for the movement and for the visibility will appear soon in the next FDS+Evac version.

In FDS+Evac, the evacuation simulation is directly affected by the fire and smoke development (see Figure 16). In Figure 17, the FED index curves describing the maximal value of agents intoxication in the area in time are shown. The index rapidly grows in both evacuation scenarios at the same time and drops down when the intoxicated agents escape (are erased from the simulation domain).

4 CONCLUSION

In this paper, we tested one sequential and ten parallel FDS simulations of smoke transfer in a road tunnel during a 10 MW fire. Parallel calculations include eight MPI simulations, one 8-threading OpenMP simulation and one hybrid MPI & OpenMP simulation. The impact of partitioning the computational domain on the simulation results reliability was investigated. All simulations led to realistic smoke transfer behaviour and confirmed that the parallel version 5.5.3 of FDS is able to provide results with reasonable precision even for simulations with a considerable number of computational meshes. The simulation results indicate that significant computational time savings can be achieved without severe impact on the simulation precision. Some specific features of particular parallel simulations were demonstrated and analysed. Further research is needed to evaluate the impact of parallelization of the computation on the results precision. Especially, study of the influence of the

numerical approach describing physical processes on mesh boundaries implemented in the current parallel FDS version is a challenging problem. Next, we evaluated the performance of the particular parallel simulations and compared them with the sequential version of the calculation. The simulation results confirmed that the MPI version of the simulation is most efficient with regard to the number of used computational cores. In comparison with the sequential version, the MPI versions show a speedup of 2 to 11 times depending on the way of domain decomposition. The performance improvement achieved by the OpenMP implementation of the calculation is not so significant (the simulation using 8 OpenMP threads reached the speedup of 1.5 times). The question whether a combination of both parallelization strategies can be beneficial requires additional testing.

We used the tunnel fire scenario used for the study of the impact of parallelization on fire simulation results and considered simple evacuation of 116 passengers from 20 cars and two buses. The use of FDS+Evac for two evacuation scenarios is illustrated to demonstrate the ability of the evacuation FDS module Evac to directly involve the related fire parameters into evacuation simulation. We add some specific remarks about selected features relevant to tunnel evacuation in fire conditions (followed from some particularities of the current version of Evac), which can be useful for FDS+Evac users. We also comment the problem of evacuees' personal settings (which must be handled properly not to distort the evacuation simulation results) and their group behaviour during tunnel evacuation.

In this research, we utilize our actual experience with analysis of current models for fire and crowd dynamics [10, 9, 11, 12, 13, 14], and testing FDS and FDS+Evac for fire simulation in various environments and evacuation simulation in the case of road tunnel fire, respectively. The results presented here indicate that proper parallelization of calaculation can have substantial impact on efficiency and accuracy of simulation of road tunnel fires as well as on reliability of modelling people evacuation. Note that reaction times of fire detection and alarm system considered in this study were relatively short to keep the total computational time of simulation acceptable considering the available computational power. In real situations, however, many other factors were observed which influence the fans activating times and smokiness of tunnel tube even before open flames appear [15], and various psychological, physiological and physical impacts on evacuees' behavior, movement and decision making were investigated (see e.g. [41, 43, 31]).

Acknowledgements

This paper was partially supported by National Science Agency (contracts VEGA 2/0184/14 and VEGA 2/0054/12) and Agency for Structural Funds of EU (research project CRISIS ITMS 26240220060, Science and Development Operational Programme). The authors would like to thank to the colleagues M. Dobrucký, J. Astaloš and P. Slížik for their technical support during calculations on HP blade cluster.

REFERENCES

[1] Betta, V.—Cascetta, F.: Numerical Study of the Optimization of Pitch Angle of an Alternative Jet Fan in a Longitudinal Tunnel Ventilation System. Tunnelling and Underground Space Technology, Vol. 24, 2009, No. 2, pp. 164–172.

[2] Borello, D.—Giuli, G.—Rispoli, F.: A CFD Methodology for Fire Spread and Radiative Effects Simulation in Longitudinal Ventilation Tunnels: Application to the Memorial Tunnel. International PHOENICS User Conference, September 23–27, 2002, Moscow 2002.

[3] Carvel, R.—Rein, G.—Torero, J.: Ventilation and Suppression Systems in Road Tunnels: Some Issues Regarding Their Appropriate Use in a Fire Emergency. Proceedings of the 2nd Int. Tunnel Safety Forum for Road and Rail, April 20–22, 2009, pp. 375–382.

[4] EGI – European Grid Infrastructure. Available on: `http://www.egi.eu/`.

[5] EMI – European Middleware Initiative. Available on: `http://www.eu-emi.eu/`.

[6] Ferng, Y. M.—Lin, C. H.: Investigating of Appropriate Mesh Size and Solid Angle Number for CFD Simulating the Characteristics of Pool Fires with Experimental Assessment. Nuclear Engineering and Design, Vol. 240, 2010, No. 4, pp. 816–822.

[7] Forney, G. P.: Smokeview (Version 5) – A Tool for Visualizing Fire Dynamics Simulator Data Volume III: Verification Guide, NIST Special Publication 1017-1C, U.S. Goverment Printing Office, Washington 2009, p. 52.

[8] Frantzich, H.—Nolsson, D.: Utrymniong Genom Tat Rok: Beteedde och Forfytting. Report 3126, Department of Fire Safety Engineering, Lund University, Sweden 2003, p. 75.

[9] Glasa, J.—Halada, L.: On Elliptical Model for Forest Fire Spread Modeling and Simulation. Mathematics and Computers in Simulation, Vol. 78, 2008, No. 1, pp. 76–88.

[10] Glasa, J.—Halada, L.: A Note on Mathematical Modelling of Elliptical Fire Propagation. Computing and Informatics, Vol. 30, 2011, No. 6, pp. 1303–1319.

[11] Glasa, J.—Valasek, L.: Study of Applicability of FDS+Evac for Evacuation Modeling in Case of Road Tunnel Fire. Research Journal of Applied Sciences, Engineering and Technology, Vol. 7, 2014, No. 17, pp. 3603–3615.

[12] Glasa, J.—Valasek, L.—Halada, L.—Weisenpacher, P.: Impact of Turned Cars in Tunnel on Modelling People Evacuation in Fire Conditions. Proceedings of 8th EUROSIM Congress on Modelling and Simulation, IEEE Computer Society (CPS), Cardiff 2013, pp. 84–89.

[13] Glasa, J.—Valasek, L.—Weisenpacher, P.—Halada, L.: Cinema Fire Modelling by FDS. Journal of Physics: Conference Series, Vol. 490, 2014, Art. No. 012067, DOI: 10.1088/1742-6596/490/1/012067.

[14] Halada, L.—Weisenpacher, P.—Glasa, J.: Computer Modelling of Automobile Fires. Chapter 9. In: Liu, Ch. (Ed.): Advances in Modeling of Fluid Dynamics. InTech Publisher, Rijeka 2012, pp. 203–228.

[15] Han, X.—Cong, B.—Li, X.—Han, L.: Effect Analysis of Fans Activating Time on Smoke Control Mode for Road Tunnel Fire. Research Journal of Applied Sciences, Engineering and Technology, Vol. 5, 2013, No. 13, pp. 3571–3575.

[16] Helbing, D.—Farkas, I.—Vicsek, T.: Simulating Dynamical Features of Escape Panic. Nature, Vol. 407, 2000, pp. 487–490.

[17] Helbing, D.—Farkas, I.—Molnar, P.—Vicsek, T.: Simulating of Pedestrian Crowds in Normal and Evacuation Situations. In: Schreckerberg, M., Sharma, S. D. (Eds.): Pedestrian and Evacuation Dynamics, Springer, Berlin 2002, pp. 21–58.

[18] Helbing, D.—Molnar, P.: Social Force Model for Pedestrian Dynamics. Physical Review E, Vol. 51, 1995, No. 5, pp. 4282–4286.

[19] Hu, L. H.—Fong, N. K.: Modelling Fire-Induced Smoke Spread and Carbon Monoxide Transportation in a Long Channel: Fire Dynamic Simulator Comparisons with Measured Data. Journal of Hazardous Materials, Vol. 140, 2007, pp. 293–298.

[20] Ingason, H.: State of the Art of Tunnel Fire Research. Proceedings of the 9th International Symposium on Fire Safety Science, Karlsruhe, Germany, 2008, pp. 33–48.

[21] Ingason, H.—Li, Y. Z.: Model Scale Tunnel Fire Tests with Longitudinal Ventilation. Fire Safety Journal, Vol. 45, 2010, pp. 371–384.

[22] Ji, J.—Fan, C. G.—Zhong, W.—Shen, X. B.—Sun, J. H.: Experimental Investigation on Influence of Different Transverse Fire Locations on Maximum Smoke Temperature under the Tunnel Ceiling. International Journal of Heat and Mass Transfer, Vol. 55, 2012, No. 17, pp. 4817–4826.

[23] Job Description Language Attributes Specification (for the gLite Workload Management System), August 2, 2011. Available on: `https://edms.cern.ch/file/590869/1/WMS-JDL.pdf`.

[24] Kelly, A.—Giblin P. E.: The Memorial Tunnel Fire Ventilation Test Program. ASHRAE Journal, February 1997.

[25] Korhonen, T.—Hostikka, S.: Fire Dynamics Simulator with Evacuation: FDS+Evac. Technical Reference and User's Guide, VTT, Finland 2009.

[26] Korhonen, T.—Hostikka, S.—Keski-Rahkonen, O.: A Proposal for the Goal and New Techniques of Modelling Pedestrian Evacuation in Fires. Proceedings of the Eight International Symposium on Fire Safety Science, 2005, pp. 557–567.

[27] Korhonen, T.—Hostikka, S.—Heliövaara, S.—Ehtamo, H.: FDS+Evac: An Agent Based Fire Evacuation Model. Proceedings of the 4th International Conference on Pedestrian and Evacuation Dynamics, Wuppertal, Germany, February 27–29, 2008, 12 pp.

[28] Korhonen, T.—Hostikka, S.—Heliövaara, S.—Ehtamo, H.—Matikainen, K.: Integration of an Agent Based Evacuation Simulation and the State-of-the-Art Fire Simulation. Proceedings of the 7th Asia-Oceania Symposium on Fire Science and Technology, Hong Kong, September 20–22, 2007.

[29] Korhonen, T.—Hostikka, S.—Heliövaara, S.—Ehtamo, H.—Matikainen, K.: FDS+Evac: Evacuation Module for Fire Dynamics Simulator. Proceedings of the 11th International Conference on Fire Science and Engineering (Interflam 2007), Interscience Communications Limited, London, UK 2007, pp. 1443–1448.

[30] Korhonen, T.—Hostikka, S.—Heliövaara, S.—Ehtamo, H.—Matikainen, K.: FDS+Evac: Modelling Social Interactions in Fire Evacuation. Proceedings of the 7th International Conference on Performance-Based Codes and Fire Safety Design Methods, Auckland, New Zealand, April 16–18, 2008, SFPE, Bethesda, MD, USA 2008, pp. 241–250.

[31] Kutilová, K.—Kučera, P.—Meinel, R.: Factors Influencing the Movement of People During Evacuation (in Czech). Proceedings of the 22nd International Conference on Fire Safety, Sdružení požarního a bezpečnostního inženýrství, Ostrava 2013, pp. 137–140.

[32] Langston, P. A.—Masling, R.—Asmar, B. N.: Crowd Dynamics Discrete Element Multi-Circle Model. Safety Science, Vol. 44, 2006, No. 5, pp. 395–417.

[33] Lin, C. H.—Ferng, Y. M.—Hsu, W. S.: Investigating the Effect of Computational Grid Sizes on Predicted Characteristics of Thermal Radiation for a Fire. Applied Thermal Engineering, Vol. 29, 2009, No. 11, pp. 2243–2250.

[34] McGrattan, K.—Baum, H.—Rehm, R.—Mell, W.—McDermott, R.: Fire Dynamics Simulator (Version 5). Technical Reference Guide (Mathematical Model). National Institute of Standards and Technology Special Publication 1018-5, October 2007.

[35] McGrattan, K.—McDermott, R.—Hostikka, S.—Floyd, J.: Fire Dynamics Simulator (Version 5). User's Guide. National Institute of Standards and Technology Special Publication 1019-5, October 29, 2010.

[36] MPI-Start and MPI-Utils, version 1.4.0, October 4, 2012. Available on: `https://devel.ifca.es/mpi-start/raw-attachment/wiki/EmiRelease/gliteMPI1.4.0/emi-mpi-1.4.0.pdf`.

[37] OpenMP – Open Multi-Processing, API Specification for Parallel Programming. Available on: `http://openmp.org/`.

[38] Open MPI – A High Performance Message Passing Library. Available on: `http://www.open-mpi.org/`.

[39] PBS – Portable Batch System. Available on: `http://www.mcs.anl.gov/research/projects/openpbs/`.

[40] Purser, D. A.: Toxicity Assessment of Combustion Products. In: SFPE Handbook of Fire Protection Engineering, 2nd edition, National Fire Protection Association, Quincy, MA, 1995, pp. 2/28–2/146.

[41] Ronchi, E.—Colonna, P.—Berloco, N.: Reviewing Italian Fire Safety Codes for the Analysis of Road Tunnel Evacuations: Advantages and Limitations of Using Evacuation Models. Safety Science, Vol. 52, 2013, pp. 28–36.

[42] Ronchi, E.—Colonna, P.—Capote, J.—Alvear, D.—Berloco, N.—Cuesta, A.: The Evaluation of Different Evacuation Models for Assessing Road Tunnel Safety Analysis. Tunelling and Underground Space Technology, Vol. 30, 2012, pp. 74–84.

[43] Ronchi, E.—Colonna, P.—Gwynne, S. M. V.—Purser, D. A.: Representation of the Impact of Smoke on Agent Walking Speeds in Evacuation Models. Fire Technology, Vol. 49, 2013, pp. 411–431.

[44] Se, C. M. K.—Lee, E. W. M.— Lai, A. C. K.: Impact of Location of Jet Fan on Airflow Structure in Tunnel Fire. Tunnelling and Underground Space Technology, Vol. 27, 2012, No. 1, pp. 30–40.

[45] Tilley, N.—Rauwoens, P.—Merci, B.: Verification of Accuracy of CFD Simulations in Small-Scale Tunnel and Atrium Fire Configuration. Fire Safety Journal, Vol. 46, 2011, No. 4, pp. 186–193.

[46] Vega, M. G.—Diaz, K. M. A.—Oro, J. M. F.—Tajadura, R. B.—Morros, C. S.: Numerical 3D Simulation of Longitudinal Ventilation System: Memorial Tunnel Case. Tunnelling and Underground Space Technology, Vol. 23, 2008, No. 5, pp. 539–551.

[47] Wang, F.—Wang, M.—He, S.—Deng, Y.: Computational Study of Effects of Traffic Force on the Ventilation in Highway Curved Tunnels. Tunnelling and Underground Space Technology, Vol. 26, 2011, pp. 481–489.

[48] Weisenpacher, P.—Halada, L.—Glasa, J.: Computer Simulation of Fire in a Tunnel Using Parallel Version of FDS. Proceedings of the 7th Mediterranean Combustion Symposium, Associazione Sezione Italiana del Combustion Institute, 2011, p. 11.

[49] Weisenpacher, P.—Halada, L.—Glasa, J.—Šipková, V.: Parallel Model of FDS Used for a Tunnel Fire Simulation. Proceedings of the International Conference ParNum 11, University of Graz 2011, pp. 96–105.

[50] Werner, T.—Helbing, D.: The Social Force Pedestrian Model Applied to Real Life Situations. Proceedings of the 2nd International Conference on Pedestrian and Evacuation Dynamics, University of Greenwich, London 2003, pp. 17–26.

Peter Weisenpacher studied theoretical physics at Comenius University, Faculty of Mathematics and Physics, Department of Theoretical Physics, Bratislava, Slovakia and received his Ph. D. in 2003. He works as research scientist at Slovak Academy of Sciences, Institute of Informatics, Department of Numerical Methods and Algorithms. His current research interests include computational fluid dynamics, fire computer simulation and parallel computing. He participates in various research projects on fire simulation.

Ján Glasa graduated in numerical mathematics in 1986, received the RNDr. (Rerum Naturalium Doctor) degree in numerical mathematics and optimization methods and algorithms at Comenius University in Bratislava, Slovakia and the C. Sc. degree (equivalent to Ph. D.) in computer science at Slovak Academy of Sciences. He works for the Institute of Informatics, Slovak Academy of Sciences in Bratislava as a senior scientist and serves as the head of the Scientific Council of the Institute. His current research interests include mathematical modelling and computer simulation of fires and parallel computing.

Ladislav Halada graduated in mathematics in 1971, received the RNDr. degree in mathematics and physics from the Faculty of Mathematics and Physics of Comenius University in Bratislava, and the C. Sc. degree (equivalent to Ph. D.) in mathematics in 1982 from the same university. He is Associate Professor from 1991. During 1972–2001 he worked on different scientific institutions and universities in Slovak Republic and also abroad. He is co-author of scientific books and numerous scientific papers.

Lukáš Valášek graduated in applied mathematics and received the Eng. degree in mathematical and computer modelling in 2012 at the Slovak University of Technology in Bratislava, Faculty of Civil Engineering. He is a Ph. D. student at the Institute of Informatics of Slovak Academy of Sciences, Bratislava, Slovakia. His major research interests include mathematical modelling and computer simulation of fires and their consequences.

Viera Šipková received the M. Sc. degree in mathematics and the RNDr. (Rerum Naturalium Doctor) degree in computer science at the Comenius University in Bratislava, Slovakia. Her research deals with parallel and distributed computing technologies. For several years she has officiated at the Vienna University, where her research efforts were focused on the high performance Fortran compiler and the automatic parallelization of scientific applications for distributed memory systems. At present she works at the Institute of Informatics of the Slovak Academy of Sciences and her main research interests include technologies for high performance computing (cluster, grid, cloud), preferring the development and porting complex scientific applications into a HPC environment. She participated in solving of many national and international research projects.